T.C.

AKDENİZ ÜNİVERSİTESİ

A NEW WAY OF DRIVING SINGLE-PHASE INDUCTION MOTOR USING SOLAR ENERGY

Mustafe Aden MUHUMED

INSTITUTE OF SCIENCES

ELECTRICAL AND ELECTRONIC

DEPARTMENT OF ENGINEERING

MASTER’S THESIS

SEPTEMBER 2022

ANTALYA

T.C.
AKDENİZ ÜNİVERSİTESİ

A NEW WAY OF DRIVING SINGLE-PHASE INDUCTION MOTOR USING SOLAR ENERGY

Mustafe Aden MUHUMED

INSTITUTE OF SCIENCES

ELECTRICAL AND ELECTRONIC

DEPARTMENT OF ENGINEERING

MASTER’S THESIS

SEPTEMBER 2022

ANTALYA

T.C.

AKDENİZ ÜNİVERSİTESİ

FEN BİLİMLERİ ENSTİTÜSÜ

A NEW WAY OF DRIVING SINGLE-PHASE INDUCTION MOTOR USING SOLAR ENERGY

Mustafe Aden MUHUMED

ELECTRICAL AND ELECTRONIC

DEPARTMENT OF ENGINEERING

MASTER'S THESIS

This thesis was unanimously accepted by the jury on 29 / 09 /2022

Prof. Dr. Selim BÖREKCİ

Prof. Dr. Ali KIRÇAY

Doc. Dr. Sıddık Cumhur BAŞARAN

ÖZET

GÜNEŞ ENERJİSİ KULLANARAK TEK FAZLI ASENKRON MOTORUNUN YENİ BİR SÜRÜŞ YOLU

Mustafe Aden MUHUMED

Yüksek Lisans Tezi, Elektrik ve Elektronik Anabilim Dalı

Danışman: Prof. Dr. Selim BÖREKCI

Eylül 2022; 36 sayfa

Tek fazlı asenkron motorlar (TFAM)'ler hem ticari hem de ev uygulamalarında yaygın olarak kullanılmaktadır. Ayrıca, kırsal alanlarda su pompalama için tek fazlı asenkron motor kullanılmaktadır. TFAM kendi kendine başlamaz. Kendi kendine başlaması için başka bir sargıya ihtiyacı vardır. Bu, yardımcı sargı olarak da adlandırılan ek bir "yardımcı sargı" eklenerek elde edilebilir. TFAM'nin başlangıç torkunu iyileştirmek için kullanılan farklı yöntemler vardır. Tek fazlı endüktans motor başlangıç torkunun iyileştirilmesi için en bilinen yöntemlerden biri kapasitörlerdir. Kondansatörsüz sistemlerde tork hızı eğrileri sınırlıdır. Kondansatörlerin ömrü sınırlıdır ve kırsal alanlarda kapasitörlerin değiştirilmesi zordur. Bu çözüm, kırsal alanlarda kondansatör kullanmanın dezavantajlarından biridir. Bu çalışmada, Tek fazlı asenkron motorların tahrik edilmesi ve tork karakteristiğinin iyileştirilmesi için iki adet inverter kullanılmış ve kapasitör kullanımı ortadan kaldırılmıştır. İki invertör arasındaki faz açısı, istenen başlangıç torkunu karşılamak için kontrol edilir. Bu tez ile tork hız eğrilerinde iyileştirmeler sağlanmaktadır. Motor tarafından sağlanan enerji, PV panellerinden, rüzgar jeneratörlerinden veya bir elektrik şebekesinden olabilir. Bu çalışmada simülasyon için MATLAB programı kullanılmıştır.

ANAHTAR KELİMELER: Fotovoltaik, Güneş, İnvertör. Kondansatör, Tek fazlı asenkron motor.

JÜRİ: Prof. Dr. Selim BÖREKCİ

Prof. Dr. Ali KIRÇAY

Doç. Dr. Sıddık Cumhur BAŞARAN

ABSTRACT

A NEW WAY OF DRIVING SINGLE-PHASE INDUCTION MOTOR USING SOLAR ENERGY

Mustafe Aden MUHUMED

Master Thesis, Department of Electrical and Electronics

Supervisor: Prof. Dr. Selim BÖREKCİ

September 2022; 36 pages

Single-phase induction motors SPIMs are widely used in both commercial and home applications. Single-phase induction for water pumping purposes is also used in rural areas where there is no electrical network. SPIM has a single winding does not start by itself. It can be changed to a two-phase motor at starting to allow it to start by itself. This can be achieved by adding an additional "starter winding," also called the auxiliary winding. There are different methods used to improve the SPIM starting torque characteristic. One of the most known methods for the improving SPIM starting torque are capacitors. The life span is limited for the capacitors, and the replacement of capacitors is difficult in rural areas. That is one of disadvantages of using capacitors. In this study, two inverters were used to drive and improve the torque characteristic of the SPIM, and the use of capacitors is eliminated. The phase angle between the two inverters is controlled to meet the desired starting torque. With this thesis, it provides improvements in torque speed curves. The energy provided by the motor can be from PV panels, wind generators, or an electrical network. A MATLAB program was used for simulation in this study.

KEYWORDS: Capacitor, Inverter, Photovoltaic, Single-phase induction motor, Solar.

COMMITTEE: Prof. Dr. Selim BÖREKCİ

Prof. Dr. Ali KIRÇAY

Assoc. Prof. Dr. Sıddık Cumhur BAŞARAN

PREFACE

One of the biggest problems for single-phase induction motors that have only one main winding is that they are not self-starting and need an external device for the purpose of starting the motor. In this thesis, a new type of driver will be used to help the motor to rotate. This new type will be an inverter, and it will be used to improve the starting torque of the SPIM without using capacitor**.**

First, I would like to thank Allah, the Almighty, for his blessings given to me during the study and for giving me the opportunity to achieve my goal. I'd like to thank my mother and family for always being there for me throughout this process.

Finally, I would like to thank the Turkish Scholarship (YTB) for supporting me throughout this education.

TABLE OF CONTENTS

ACADEMIC STATEMENT

I state that this study, titled " A new way of driving a single-phase induction motor using solar energy," which I submitted as a master’s Thesis, was written in accordance with academic rules and ethical values, and I declare that I have indicated the source of all information that does not belong to me in this thesis.

29 / 09 / 2022

Mustafe Aden MUHUMED

SYMBOLS AND ABBREVIATIONS

Symbols

Z_f	:forward impedance
Z_b	: backward impedance
R_f	: forward resistance
R_f	: backward resistance
S	: Slip
ω_{sync}	: synchronous speed
τ_{ind}	: induced torque
P_{ag}	: air-gap power
$P_{ag,f}$	: air-gap power forward
$P_{ag,b}$	: air-gap power backward
τ_{load}	: load torque
P_{out}	: output torque
η	: Efficiency
A	: Ampere
V	: Voltage
Kw	: Kilowatt
Ncells	: cells per module

Abbreviation

SPIM	: Single Phase Induction Motor
DC	: Direct Current
AC	: Alternative Current
PV	: Photovoltaic
PWM	: Pulse Width Modulation.
SPWM	: Sinusoidal Pulse Width Modulation.
MSPWM	: Modified Sinusoidal Pulse Width Modulation.
IGBT	: Insulated-gate bipolar transistor
GTOs	: gate turn-off thyristor
THD	Total Harmonic Distortion
VSI	Voltage Source Inverter
Vmp	Maximum output voltage (V)
Imp	Maximum output Current (A)
Voc	Open Circuit Voltage
Isc	Short Circuit Current

LIST OF TABLES

LIST OF FIGURES

1. INTRODUCTION

1.1. Introduction

Single-phase induction motor (SPIM) is used in fans, washing machines, and water pump systems. As an example, it is commonly used in water irrigation systems. Water resources are essential for satisfying human needs, protecting health, and ensuring food production, energy, and the restoration of ecosystems, as well as for social and economic development and sustainable development. Remote water pumping systems are a key component in meeting this need (Anwari 2009). In some areas, there is no electrical power. To provide energy to water pumps, PV energy systems are utilized. The energy is provided by PV panels. The output of the PV solar energy is direct current (DC). For this reason, power inverters are used to convert the direct current into alternative current (AC).

Single-phase induction motor with one stator winding does not produce any starting torque. The motor to start rotating, some configuration is needed so that the motor can provide a starting torque. Adding an auxiliary winding to the stator in addition to the main winding and starting the motor as a two-phase machine is the simplest way to start a single-phase induction motor. The axes of the two windings are 90 electrical degrees apart from one another when they are installed in the stator. In its operating state, a single-phase induction motor can produce torque using only its main winding. The auxiliary winding can be removed from the circuit as the motor accelerates. A centrifugal switch is connected to the auxiliary circuit of most motors to accomplish this. A centrifugal switch activates and separates the auxiliary winding from the supply at around 75% of the synchronous speed. (P. Sen 2007.)

To change the torque speed characteristics of SPIM capacitors are used. The main advantage of usage of capacitors are to improve the motors starting torque. The life span is limited for the capacitors, which is the disadvantage of using capacitors in these solutions. In this study, two inverters were used to drive and improve the torque characteristic of the SPIM, and the use of capacitors is eliminated. The phase angle between the two inverters is controlled to meet the desired starting torque. With this thesis, it provides improvements in torque speed curves. The energy provided by the motor can be from PV panels, wind generators, or an electrical network. Figure 1.1 shows the proposed system of this study.

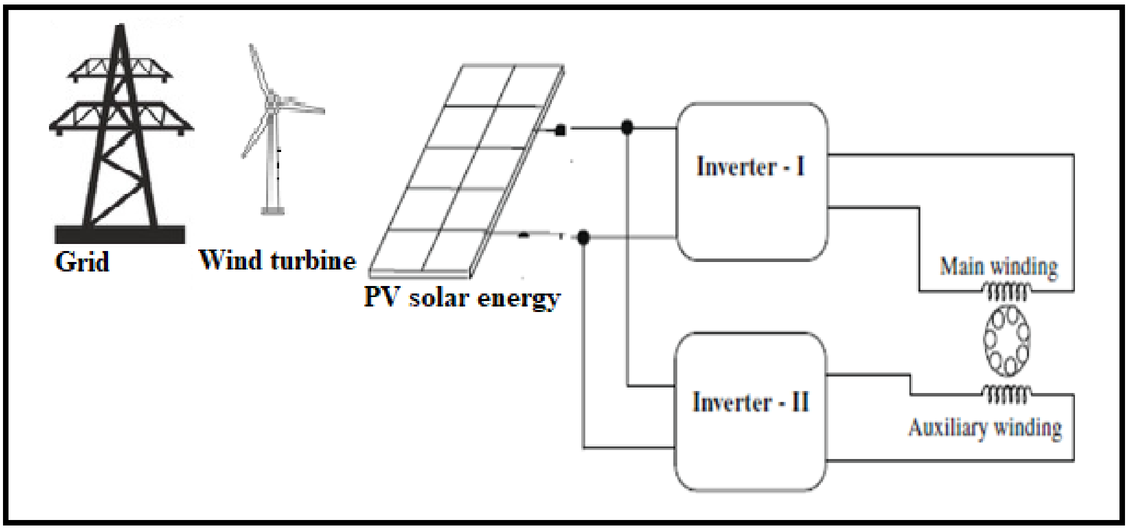

Figure 1.1. Configuration of a proposed system

1.2. Problem statement

A single-phase induction motor with one main winding does not start by itself. It can be modified to a two-phase motor at starting to allow it to start by itself. This can be achieved by adding an additional "starter winding," also called the auxiliary winding. There are different methods used to make SPIMs self-starting. The capacitor is connected in series with the auxiliary winding to improve the starting torque of SPIM. The lifespan of the capacitors' that are used for SPIM is short. This is one of the disadvantages of capacitor-start induction motors.

A single-phase induction motor is used for water pumping systems in agricultural irrigation. It is difficult to find electric power and replacing a capacitor becomes problem in rural areas particularly in Africa.

1.3. Objective

The goal of this research is to design a new way of driving single-phase two winding induction motors by using two voltage sources without capacitors. These two voltage sources are used as power source for the main winding and the auxiliary winding of the SPIM.

1.4. Scope

Designing two inverters and a solar system for driving a single-phase induction motor was done using the MATLAB simulation program.

1.5. Outline of the thesis

Chapter one is the introduction to the thesis, and it will give information about the topic such as single-phase induction motors, inverters and solar. Also, it talks about the problem statement, the objectives of the thesis, and the scope of the thesis.

Chapter two is the literature review, and it will give information about the research, papers, or articles that are related to this topic.

Chapter three is the methodology, and it will contain the working principles of solar and single-phase induction motors.

Chapter four revolves around the proposed technique of designing, calculating, and simulating the thesis by using MATLAB simulation.

Chapter 4 is called "Results and Discussion," and it talks about the outcomes and results of a study.

The summary of the main points of the research will be in Chapter 5, which is the conclusion.

2. LITERATURE REVIEW

This chapter will contain the literature review of the thesis by describing the title of the paper shortly, the program or software, and the topologies that are used. Also, it will contain the results that were found. The summaries of the main sources of the articles and the research are given below.

By (Saini 2017), the performance of solar-fed single-phase induction motor drives for water pumping systems using the MATLAB program was examined. The power provided to the SPIM can be split into two distinct topologies. The output of the photovoltaic solar energy is connected to a DC-to-DC boost converter in the first topology to raise the Solar's output voltage. This DC output voltage is transformed to an AC power supply and provided to the single-phase induction motor via an inverter. The output DC voltage from the solar energy is directly connected into the inverter without increasing the voltage, and the inverter's output is connected to the motor in the second topology. The total harmonic distortion (THD) of the main winding current and the speed of a single-phase induction motor are used to compare the performance of these two topologies. The THD of the single-phase induction motor's primary winding current is found to be 4.34 percent for the single stage converter and 94.97 percent for the two-stage converter. This means that the THD on the first topology is 21.88 times greater than on the second topology. For the first topology, the rotor speed of the motor is 1000 rpm, while the output rotor speed in the second topology is 1875 rpm. In this paper, they suggested that using the second topology, which is to directly feed the output of the solar panel into the inverter, is better than using the dc-to-dc converter to increase the voltage of the solar panel.

Nandha kumar vd. (2019), Using MATLAB simulation and hardware results obtained from a PIC microcontroller, a SPIM driven by a multi-stage power conversion circuit has been modeled and developed. There are two stages that are used in this paper. In the first stage, a DC-to-DC boost converter is used after filtering to maximize the output voltage of the solar power. In the second stage, to achieve high performance at various operating speeds, a voltage source inverter with an open loop sub synchronous speed was used. To control the output frequency and voltage of VSI, a single-phase pulse-width modulation (PWM) technique is used. The amount of power required by the load depends on the operating voltage of the solar energy. In general, the change in temperature and the radiation of the sun reduce or decrease the maximum power point of the sun. If the MPP reduces the speed of the single induction motor, it becomes very low. So, to get maximum power point tracking perturb and observable technique are used. The hardware circuit of the system consists of a PIC microcontroller, inverter circuit with a single-phase induction motor, rectifier circuit, and regulator voltage. The results obtained from this paper indicate that there is more fluctuation or distortion in the output voltage, but there is less fluctuation in the current. The harmonics in the output voltage and current are large, so to reduce the harmonic filter circuit, an artificial intelligence method is used to generate the pulses for IGBT.

Vtas and Pal (2017) In this paper, they designed a solar photovoltaic system feeding single-phase induction motor drivers for pumping water using a MATLAB program. There are three steps of power conversation in the circuit. In the first step, a buck boost DC-to-DC convert is used to increase the output voltage of the solar. To control the DC-to-DC conversion, a INC MPPT controller was used. In the second step, voltage source inverters (VSI) have been used to convert the DC output voltage into AC. To control the DC-to-AC conversion, a V/F controller is employed. In a third step, a bidirectional DC-to-DC converter is utilized between the single-phase voltage source inverter and the battery bank. This study contains a 1500W, 230V, 50Hz, and 4-pole single-phase induction motor, and 356V, 45A, and 1600W output solar power have been used. The simulation results show that the capacitor start motor has 1.96% and 0.69% total harmonic distortion in voltage and current, respectively. For a split-phase induction motor, it has 2.01% and 0.26% total harmonic distortion in voltage and current, respectively. The starting performance of the capacitor-start induction motor is better than the split-phase induction motor. Also, the simulation results show that the losses in the start capacitor motor are less than the losses in the split-phase induction motor.

In their study Thomas and Mathew (2014) used a single-source, five-level inverter with a single-phase induction motor powered by solar energy. In this article, there are two types of power supply for the inverter. In type one, when the output voltage of the solar panel is increased by using a DC-to-DC boost converter, it is directly connected to the inverter. In type 2, when there is no output voltage solar energy available, a battery supplies power to the five-level inverter. This system consists of solar photovoltaic energy, a boost converter, battery, and single-phase induction motor. The perturb and observe P&O algorithm was used to track the maximum power point of the solar panel. Also, boost converters have been used for MPPT applications since the boost converter provides protection for the photovoltaic solar energy by blocking the reverse current flow to the solar power. In this research, a single-source five-level inverter is used to convert the output DC voltage of solar energy into AC voltage. The reason that they used a single-phase, five-level inverter was to reduce the total harmonic distortion (THD), switching losses, and improve the inverter's efficiency. The single-source five-level inverter is controlled by using a PWM control approach.

Ahmed vd. (2018), This paper demonstrates a five-level inverter and its basic operation using the MATLAB software tool. In addition, the performance and modeling of a capacitor-start, capacitor-run single-phase induction motor when linked to a multilevel inverter are shown in this study. The inverter that they used is a five-level single-phase pulse width modulated (PWM) inverter. They proposed a switching inverter with two switching groups. The first is set to the line frequency, while the second is set to the switching frequency. The multilevel inverter produces current with the least overall harmonic distortion, according to the simulation results.

Foito vd. (2014). A single-phase asynchronous motor with photovoltaic solar energy for a water pump system is discussed in this study. MATLAB software was utilized to generate several simulation results. The perturb and observe MPPT approach was used to extract the Solar’s maximum power point. Photovoltaic solar energy, a DC-to-DC converter, an AC to DC inverter, and a single-phase induction motor with a water pumping system are the study's system components. They use a DC-to-DC converter to boost the DC output voltage of solar energy. The flow of the centrifugal pump was controlled using a diametrical inversion (DI) controller.

Kumar and Dhal (2015) calculated the dynamic and steady-state operation of a single-phase induction motor using the MATLAB Simulink software. The induction motor mentioned in this paper is a star capacitor-run induction motor with variable capacitor values and the same voltage supply frequency. When the SPIM is not loaded and when it is fully loaded, they use a constant frequency and vary the capacitor value. They also employed open- and closed-loop systems. power supply, power electronic converter, pulse generator, and motor are the components of this article. The power supply for the single-phase induction motor was an inverter with two cascade bridges. The result of the paper shows that THD values under open loop systems for three, five, and seven level inverters are 36.13%, 18.32%, and 17.10%, respectively. And under a closed loop system, THD values are 32.54%, 15.35%, and 15.16% for three, five, and seven level inverters, respectively.

Ugale and Panse (2015) described a single-phase induction motor driven by solar photovoltaics for a water pumping system using a MATLAB application. Solar, a power conditioner, a single-phase induction motor, and water pumping equipment are the components in this system. There are two topologies in this system. In the first topology, the solar output power is directly linked to the single-phase induction motor without the use of a DC-to-DC converter. This is only possible if the solar panel's output voltage is high enough. The output voltage of the solar is boosted in the second topology using a DC-to-DC converter since the output voltage of the solar is insufficient to connect to the inverter. An inverter is used to feed SPIM in both topologies. The pulse width modulation approach is utilized in the simulation to control the output current and voltage. The major goal of this study was to provide low-cost water in rural areas.

Most of the articles mentioned above are about a single-phase induction motor drive for a water pumping system that gets power from solar photovoltaic. Only The difference between them is the topologies and the level of single-phase inverter that are used. The goal of this study is to drive the single-phase induction motor by using two different voltage sources, one for the main winding and the other for the auxiliary winding, to improve the starting torque of the single-phase induction motor, a phase angle is added to one of the voltage sources.

3. MATERIAL AND METHOD

3.1. Material

3.1.1. Solar cell

The solar cell is the basic component of a PV system. Solar cells are capable of directly transforming the energy from sunlight into electricity**.** Solar cells generate electricity using a quantum-mechanical mechanism known as the "photovoltaic effect"**.** (Rashid 2014)**.** Figure 3.1 shows a typical commercial silicon solar cell.

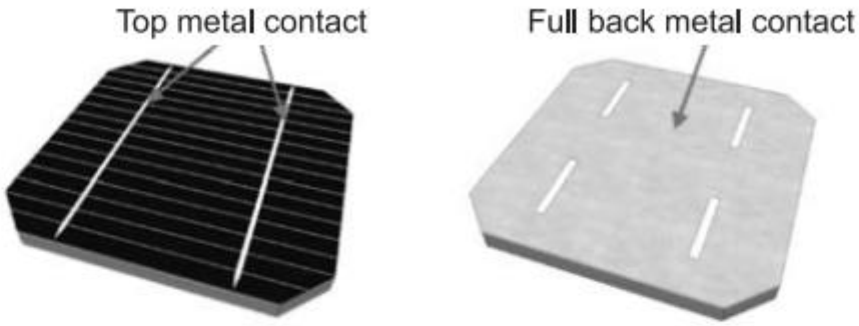

Figure 3.1. Front side and back side of a silicon solar cell

3.1.1.1. Working Principle of photovoltaic solar energy

The terminals of the solar cell generate current and voltage when exposed to sunlight. The amount of electricity produced by a solar cell is proportional to the amount of incident sunlight. The electricity produced by a solar cell is dependent on the amount of light, the area of the cell, and the angle of light incidence. The greater the intensity of sunlight, the more electricity a solar cell generates. Increasing the area of a solar cell increases the current it generates. When sunlight falls perpendicular to the front surface of the solar cell, the solar cell produces its maximum power or voltage. (Solanki 2013)

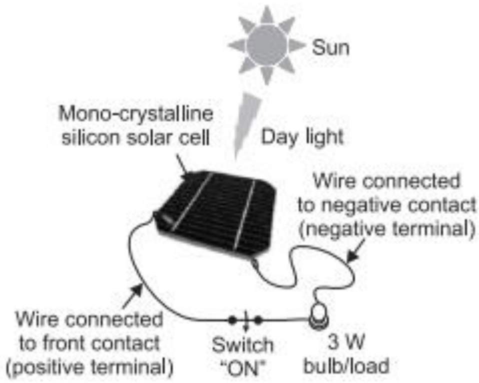

Figure 3.2. Solar cell with terminals and load

Semiconducting components absorb photons from sunlight that hit the solar cell's front surface. There are produced free electron-hole pairs. Positive charge is associated with holes, while negative charge is associated with electrons. Electrons and holes close to the junction are segregated from one another when a solar cell is linked to a load. At the positive terminal (anode), holes are gathered, and at the negative terminal, electrons (cathode). The separation of negative and positive charges results in the development of electric potential at the terminals. Due to the different electric potentials at the terminals, there will be a voltage across the terminals. The current in the circuit is powered by the voltage generated at a solar cell's terminals. DC current, often known as direct current, will flow through the circuit (Solanki 2013).

3.1.1.2. The Equivalent Circuit for a PV Cell and Module

The comparable PV solar cell circuits come in a variety of forms. The only difference between these circuits is the quantity of circuit elements. The most basic is the PV solar cell's single diode equivalent circuit, which consists of a current source or photo current source connected in parallel with a nonlinear diode, a series Rs representing internal losses, and a parallel (shunt) Rsh resistance with the diode to account for leakage current to the ground (Foito vd. (2014). As shown figure 3.3.

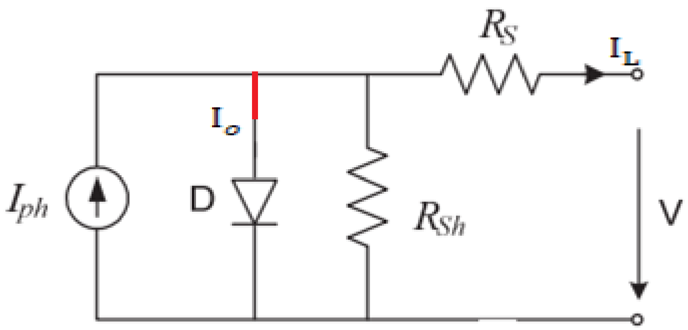

Figure 3.3. Photovoltaic equivalent circuit

$$\mathrm{I_{ph}} = \mathrm{I_L} - \mathrm{I}_o \left[\exp\left(\frac{\mathrm{q(V + R_S I_L)}}{\mathrm{nkT}}\right) - 1\right] - \frac{\mathrm{V + R_S I_L}}{R_{Sh}} \tag{3.1}$$

Where $\mathrm{I_L}$ denotes the current due to solar radiation, $\mathrm{I_o}$ the saturation current, $\mathrm{R_{sh}}$ is the resistance due to leakage current through the p-n junction, q the electron charge (1.6022e-19 C), k the Boltzmann constant (1.3806e-23 J.K-1), T the cell temperature and n the PN junction ideality factor.

3.1.1.3. I-V, P-V characteristics of PV Cell

The photovoltaic panels Voltage and current depends on the temperature and the irradiance, increasing irradiance leads to an increased current and slightly increased voltage. increasing the temperature reduces the voltage and the current output of the solar. Figure 3.4a and 3.4b show the I-V and P-V characteristics curve of the photovoltaic cell respectively at constant temperature and radiance. (Mohamed 2015).

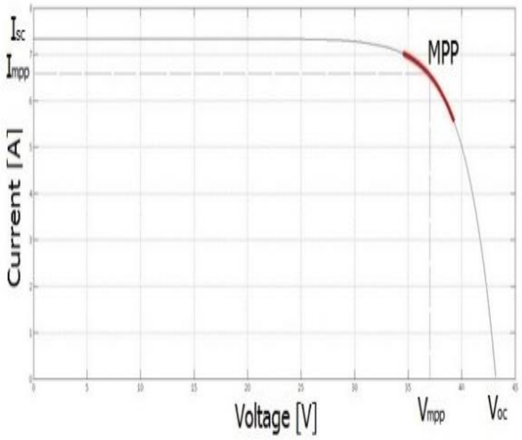

a)

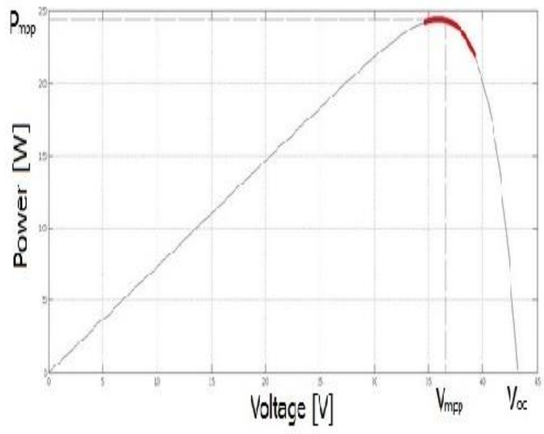

b)

Figure 3.4. a) I-V characteristics curve; **b)** P-V characteristics curve

3.1.2. Principle operation of a single-phase inverter

Inverters are the parts of a circuit that change DC to AC. Inverters convert power from a DC source to an AC load. The objective is to generate AC voltage. when there is only one source of direct current (DC). Inverters can be used to supply power to ac appliances from a car battery, as a backup power supply (UPS), and to control the speed of an ac motor drive. As shown in Fig. 3.5a, the full-bridge converter is the most basic way to change DC to AC. By closing and opening switches in sequence, a DC input can be turned into an AC output. The output voltage Vo can be positive Vdc, negative Vdc, or zero, depending on which switches are closed. S2 and S3, as well as S1 and S4, shouldn't be closed simultaneously. Otherwise, there would be a short circuit across the DC source. Actual switches do not instantly turn on or off. As a result, switching transition times need to be considered when controlling the switches. A short circuit across the dc voltage source, often known as a shoot-through fault, will occur when switch "on" times overlap. Blanking time is the amount of time that can be used for switching. (Hart 2011). The corresponding circuits for switch combination are shown in Figure 3.5 b to e.

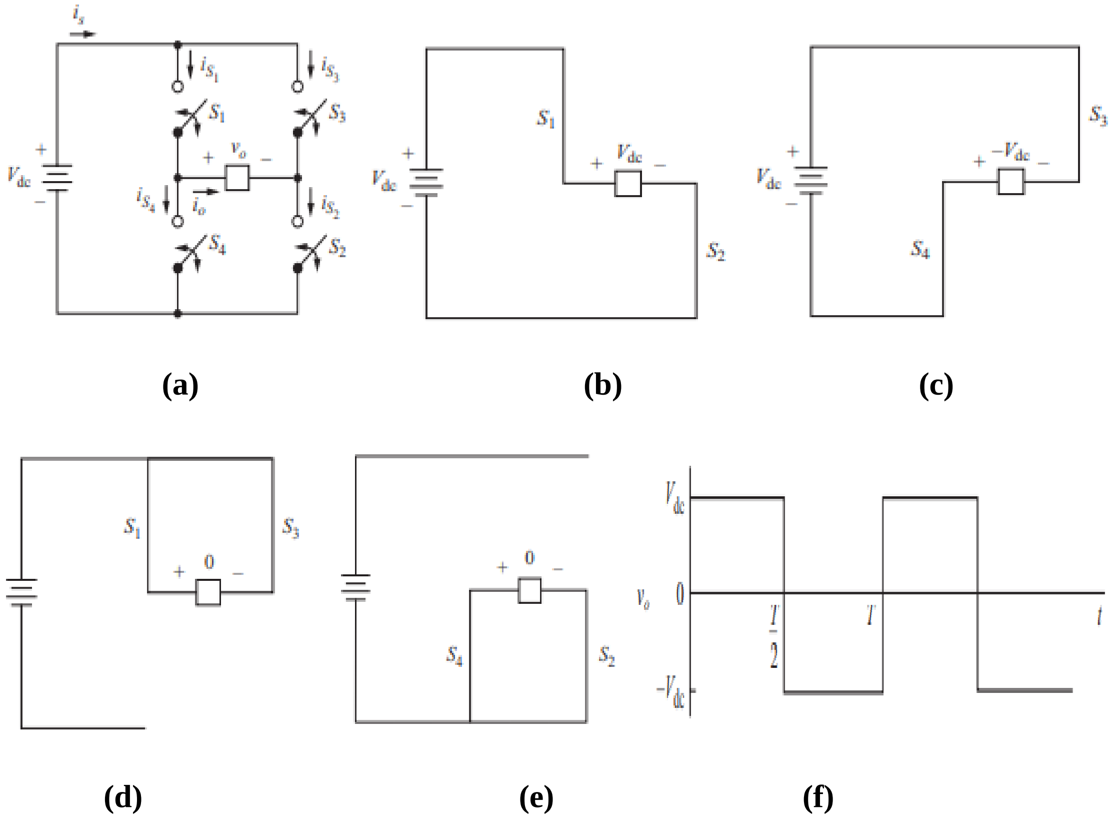

Figure 3.5. a) Full-bridge inverter; **b)** S1 and S2 closed; **c)** S3 and S4 closed; **d)** S1 and S3 closed; **e)** S2 and S4 closed; **f)** Output voltage of full bridge inverter

3.1.3. Pulse Width Modulation

In many industrial applications, controlling the output voltage of inverters is necessary to deal with fluctuations in dc input voltage, to regulate inverter voltage, and to meet the constant voltage and frequency. The inverter gain can be varied using a different method. The most effective technique to adjust the gain and output voltage is to use PWM control inside the inverters. (R. N. Muhammad 2014).The pulse width is modified to manage the inverter output voltage in single PWM control, and there is only one pulse half every cycle. Gating signals are formed by comparing the rectangular reference signal to the triangular carrier wave. The fundamental frequency of the output voltage is determined by the frequency of the reference signal (Peddapelli 2016)**.** The gate control signals in sinusoidal pulse width modulation (SPWM) are formed by comparing a sinusoidal reference voltage signal (V_{sine}) to a high-frequency triangular carrier voltage signal (V_{tri}). Figure 3.6 represents a triangular carrier signal and a sinusoidal reference signal. The output is $+V_{dc}$ when the instantaneous value of the sine reference is greater than the triangular carrier, and $-V_{dc}$ when the reference is smaller than the carrier (Youssef (2020).).

$$\text{u} = +V_{dc} \quad when \quad v_{sine} > V_{tri} \qquad \text{at} \quad S_1 \text{ and } S_2 \text{ are on} \qquad (3.2)$$

$$u = -V_{dc} \;\; when \;\; v_{sine} < V_{tri} \qquad \text{at} \qquad S_3 \text{ and } S_4 \;\; are\ on$$

This type of PWM is called bipolar because the output changes between $+V_{dc}$ and $-V_{dc}$.

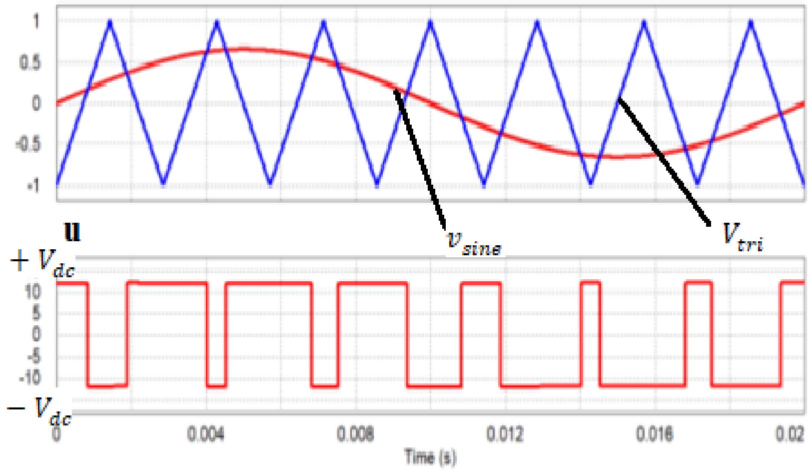

Figure 3.6. PWM signal with sine wave reference and triangle wave carrier

3.1.4. Single Phase İnduction Motors

A single-phase induction motor simple in construction, inexpensive and reliable. Drills, blowers, elevators, cordless drills, vacuum cleaners, machine tools, and pumps are examples of industrial and domestic electric motors that use it. (Iqbal 2021) The single-phase induction motor's constructional descriptions are displayed in figure 3.7.

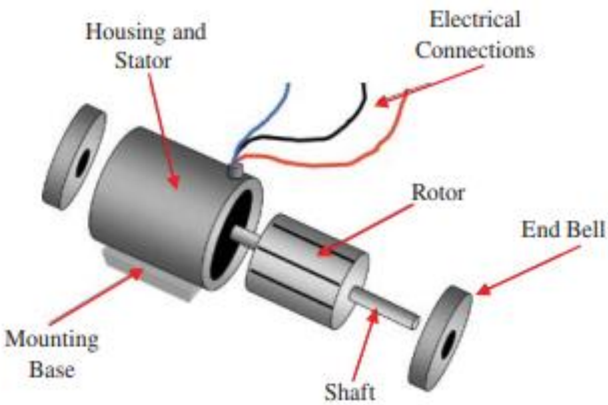

Figure 3.7. Construction of the single-phase induction motor.

3.1.4.1. Working Principles of Single Phase İnduction Motors

In comparison to three-phase induction motors, single-phase induction motors do not self-start. However, as illustrated below, a torque is instantaneously produced in the motor when the rotor is initially supplied a specific torque in either direction. After that, the motor runs to its final speed, which is always slower than its synchronous speed. The double-field revolution theory now explains this.

Suppose that the current provided to the stator winding is as

$$\imath_m = I_m \cos(\omega t) \tag{3.3}$$

As seen in Figure 3.8, this current generates sinusoidal mmf along the axis of the stator, which is expressed as

$$N\imath_m = NI_m \cos(\omega t) = F_m \cos(\omega t) \tag{3.4}$$

Where N is the effective number of stator winding turns and ω is the stator supply current's angular frequency.

The mmf along the rotor position θ is given by:

$$F(\theta, t) = J\cos(\theta) = F_m \cos(\omega t)\cos(\theta) \tag{3.5}$$

The Eq. (3.4) can be written as

$$F(\theta, t) = \frac{F_m}{2}\cos(\omega t - \theta) + \frac{F_m}{2}\cos(\omega t + \theta)$$

$$\begin{aligned} F(\theta, t) &= F_f + F_b \\ F_f &= \frac{F_m}{2}\cos(\omega t - \theta) \\ F_b &= \frac{F_m}{2}\cos(\omega t + \theta) \end{aligned} \tag{3.6}$$

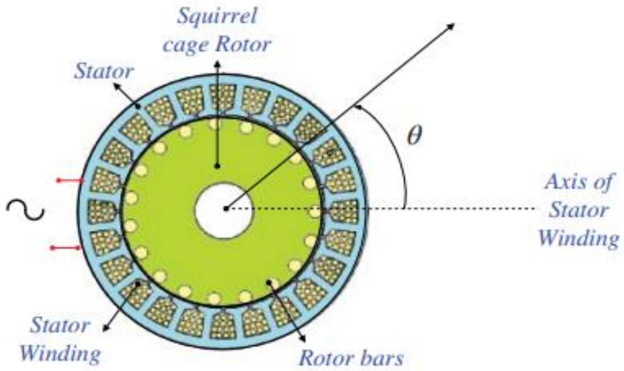

Figure 3.8. Cross-sectional view of a single-phase induction motor

According to the double revolving theory, the net mmf is divided into two fluxes, the forward flux (Ff) and the backward flux (Fb). Even though they revolve in different directions, the two mmfs are rotational in nature and rotate at an angle of ω. As a result, the net field has a pulsing rather than rotating aspect. While the position changes, the amplitude stays constant. The flux is created by the mmf. A forward-rotating component and a backward-rotating component make up the resulting flux. Figure 3.8 displays the fluxes' positions at various points in time. At a fixed point, the flux is shown to vary the amplitude. A pulsing flux is the name given to this kind of flux. **(**Iqbal 2021).

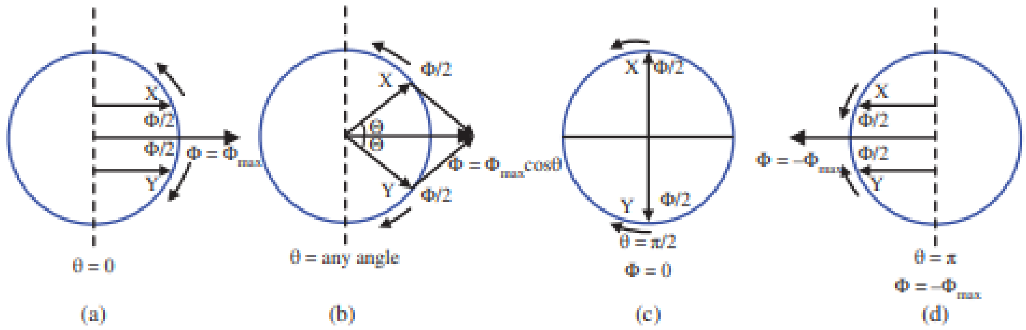

Figure 3.9. The flux that was produced in relation to the angle

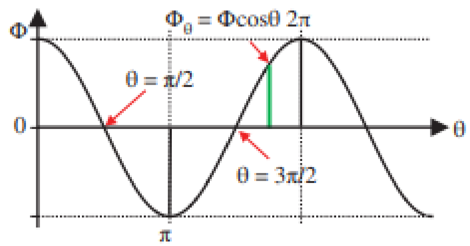

Figure 3.10. Variation of flux with angle

3.1.4.2. Single-phase induction motor equivalent circuit

A stationary pulsating magnetic field can be resolved into two rotating magnetic fields, each of comparable amplitude but spinning in opposite directions, using the double-revolving-field method of single-phase induction motors. Each magnetic field is responded to separately by the induction motor, and the machine's net torque is the sum of the torques induced by each magnetic field. . (S. Chapman 2012)**.** figure 3.10a shows the equivalent circuit of the single-phase induction motor. The equivalent circuit can be extended to include the effects of two counterrotating fields of constant magnitude using the double-revolving field theory. The magnitudes of the forward and backward resultant mmf fields are each half that of the pulsating field at standstill. As a result, the rotor-equivalent circuit can be divided into two parts. As illustrated in figure 3.10b, the equivalent circuit of a single-phase induction motor is made up of the series connection of forward- and backward-rotating field equivalent circuits. The motor's equivalent circuit must be adjusted when it has been brought up to speed using an auxiliary winding and is running in the direction of the forward rotating field at a slip s, as shown in figure 3.10c. As a result, in the forward equivalent circuit, the rotor resistance is $0.5R'_2$ /s. The difference in speed between the rotor and the backward-rotating field is also 2 - s, because the rotor rotates at a speed that is s slower than the forward-rotating field. As a result, in the analogous backward circuit, the rotor resistance is represented by $0.5R_2' /(2-S)$. (T. Gonen 2011).

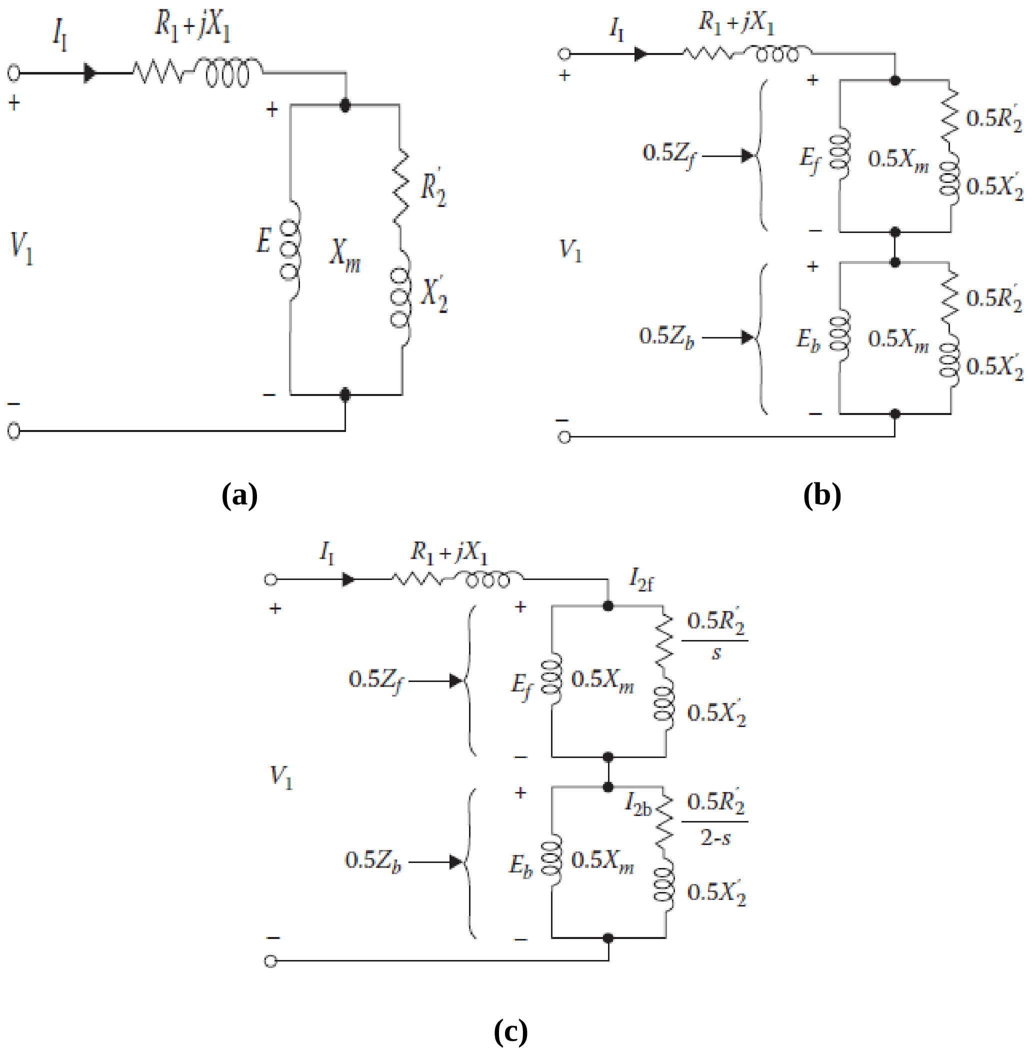

Figure 3.11. a) Equivalent circuit of SPIM; **b)** Configuration at standstill; **c)** Modified configuration at standstill

Where **R1** is the stator winding resistance, **X1** is the stator winding's leakage reactance. The magnetizing reactance is denoted by **Xm** and **R'2** rotor resistance.**X'2** rotor leakage reactance.

The following are the impedances forward and backward fields equations and it drives from figure 3.10c.

$$Z_f = R_f + jX_f = \frac{jX_m\,(R_2' /S + jX_2')}{jX_m + (R_2' /S + jX_2')} \tag{3.7}$$

$$Z_b = R_b + jX_b = \frac{jX_m\,(R_2'/(2-S) + jX_2')}{jX_m + (R_2'/(2-S) + jX_2')} \tag{3.8}$$

$$I_1 = \frac{V_1}{R_1 + jX_1 + 0.5Z_f + 0.5Z_b} \tag{3.9}$$

$$P_{g,f} = {I_1}^2(0.5R_f) \tag{3.10}$$

$$P_{g,b} = I_1^2(0.5R_b) \tag{3.11}$$

$$P_g = P_{g,f} - P_{g,b} \tag{3.12}$$

$$T_{d,f} = \frac{P_{g,f}}{\omega_s} \tag{3.13}$$

$$T_{d,b} = \frac{P_{g,b}}{\omega_s} \tag{3.14}$$

$$T_d = \frac{P_g}{\omega_s} \tag{3.15}$$

$$P_d = P_{mech} = T_d * \omega_m \tag{3.16}$$

The torque speed characteristic curve only for main winding SPIM. The MATLAB program code is used for drawing this curve by using the above equations (3.2) to (3.11). by using a typical load SPIM as example. The code will be mentioned in the **appendix (A).**

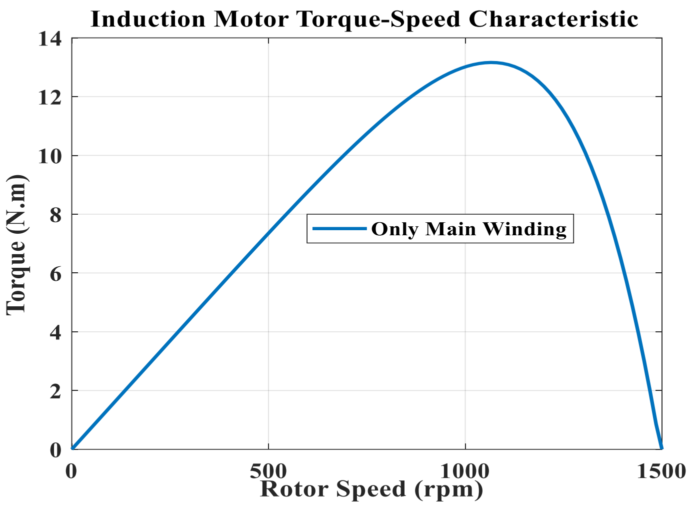

Figure 3.12. Torque-speed characteristic only main winding SPIM

3.1. Method

3.1.1. Torque Speed characteristics and Equivalent Circuit of Capacitor-star Induction Motor

The equivalent circuit of a capacitor-start single-phase induction motor that gets power from only one voltage source is illustrated in Figure 3.12. The voltage source that supplies power to both the main winding and auxiliary winding is denoted by (Vs). The capacitor is connected in series with an auxiliary winding to create a phase shift.

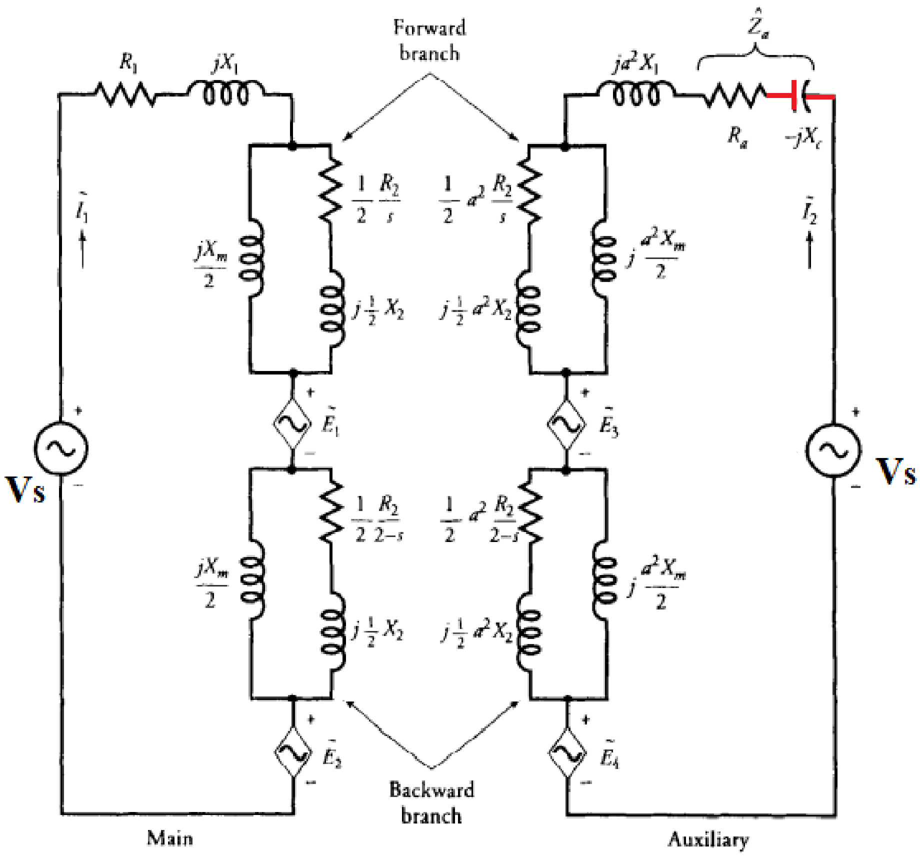

Figure 3.13. Equivalent circuit of the main winding and auxiliary windings of a capacitor-start induction motor

The below Equations are derived from the above equivalent circuit of the Capacitor-start induction motor.

Impedance of an auxiliary winding in a split-phase motor

$$Z_a = R_a \tag{3.17}$$

Impedance of the auxiliary winding on an induction motor with a capacitor start

$$Z_a = R_a - jX_c \tag{3.18}$$

The main winding's forward and backward impedances are

$$Z_f = R_f + jX_f = \frac{j0.5X_m\ (0.5R_2'\ /S\ +\ j0.5X_2')}{j0.5X_m +\ (0.5R_2'\ /S\ +\ j0.5X_2')} \tag{3.19}$$

$$Z_b = R_b + jX_b = \frac{j0.5X_m\ (0.5R_2'\ /(2-S\ ) + j0.5X_2')}{j0.5X_m + (0.5R_2'\ /(2-S\ ) + j0.5X_2')} \tag{3.20}$$

The induced emfs in the main winding by its forward and backward revolving fields are as follows:

$$E_{fm} = I_1\, Z_f \tag{3.21}$$

$$E_{bm} = I_1\, Z_b \tag{3.22}$$

The induced emfs in the auxiliary winding due to its forward and backward revolving fields are as follows:

$$\mathrm{E_{fa}} = \mathrm{I_2\ a^2 Z_f} \tag{3.23}$$

$$\mathrm{E_{fb}} = \mathrm{I_2\ a^2 Z_f} \tag{3.24}$$

The induced emf in the main winding by the forward revolving field of the auxiliary winding must lag the induced emf in the auxiliary by 90° since the main winding is electrically 90° ahead of the auxiliary winding. Additionally, the main winding's induced emf must be 1/a times that of the auxiliary's winding. This is,

$$\mathrm{E_1} = -\mathrm{j}\frac{1}{\mathrm{a}}\mathrm{E_{fa}} = -\mathrm{jaI_2Z_f} \tag{3.25}$$

Likewise, the auxiliary winding's field of backward rotation causes an induced emf in the main winding that must be 90 degrees ahead of the induced emf in the auxiliary winding. Thus,

$$\mathrm{E_2} = \mathrm{j}\frac{1}{\mathrm{a}}\mathrm{E_{ba}} = \mathrm{jaI_2Z_b} \tag{3.26}$$

Similarly, induced emfs in the forward and reverse branches of the auxiliary winding are caused by the forward and reverse revolving fields of the primary winding.

$$E_3 = jaI_1Z_f \tag{3.27}$$

$$E_4 = -jaI_1Z_b \tag{3.28}$$

Because all of the induced emfs are now known, applying Kirchhoff's voltage law to the coupled circuit produces

$$I_1\,(R_1 + jX_1) + E_{fm} + E_{bm} + E_1 + E_2 = V_1 \tag{3.29}$$

$$\mathrm{I}_2\,(\mathrm{Z}_\mathrm{a} + \mathrm{j}\mathrm{a}^2\mathrm{X}_1) + \mathrm{E}_\mathrm{fa} + \mathrm{E}_\mathrm{ba} + \mathrm{E}_3 + \mathrm{E}_4 = V_1 \tag{3.30}$$

The following equations can be expressed simply when the induced emfs have been substituted for

$$I_1\,Z_{11} + I_2\,Z_{12} = V_1 \tag{3.31}$$

$$I_1\,Z_{21} + I_2\,Z_{22} = V_1 \tag{3.32}$$

Where

$$Z_{11} = R_1 + Z_f + Z_b + jX_1 \tag{3.33}$$

$$Z_{12} = -ja[\,Z_f - Z_b\,] \tag{3.34}$$

$$Z_{21} = ja[\,Z_f - Z_b\,] \tag{3.35}$$

$$Z_{22} = Z_a + a^2[Z_f + Z_b + jX_1\,] \tag{3.36}$$

The currents flowing through the main and auxiliary windings are

$$I_1 = \frac{V_1[\, Z_{22} - Z_{12} \,]}{Z_{11}\, Z_{22} - Z_{12}\, Z_{21} \,]} \tag{3.37}$$

$$I_2 = \frac{V_1[\, Z_{11} - Z_{21} \,]}{Z_{11}\, Z_{22} - Z_{12}\, Z_{21} \,]} \tag{3.38}$$

The line current

$$I_L = I_1 + I_2 \tag{3.39}$$

the power that is provided to the motor is

$$P_{in} = Re\left[V_1 \; I_L{}^{*}\right] = V_1\, I_L \, \cos\theta \tag{3.40}$$

Where θ is the amount by which the line current lags behind the applied voltage.

The copper losses for each stator winding are

$$P_{sce} = I_1{}^2 R_1 + I_2{}^2 R_a \tag{3.41}$$

Air-gap power generated by the forward-rotating field of the main winding.

$$\begin{aligned} P_{agfm} &= Re\left[\left(E_{fm} + E_1\right) I_1{}^{*}\right] \\ &= Re\left[\left(I_1{}^2 - jaI_1{}^{*} I_2\right) Z_f\right] \end{aligned} \tag{3.42}$$

Air-gap power generated by the forward revolving field of the auxiliary winding.

$$\begin{aligned} P_{agfa} &= Re\left[\left(E_{fa} + E_3\right) I_2{}^{*}\right] \\ &= Re\left[\left(I_2{}^2 \mathrm{a}^2 - jaI_1\, I_2{}^{*}\right) Z_f\right] \end{aligned} \tag{3.43}$$

The net power of the air gap due to both forward revolving fields is

$$P_{agf} = P_{agfm} + P_{agfa}$$

$$= I_1{}^2 + a^2 I_2{}^2) R_f + 2aI_1 I_2 R_f \sin\theta \quad (3.44)$$

Where $I_1 = I_1 \angle\theta_1, I_2 = I_2 \angle\theta_2 \;\; and\; \theta = \theta_2 - \theta_1$

The net power of the air gap due to both backward revolving fields is

$$P_{agb} = Re\left[\left(E_{bm} + E_2\right) I_1{}^{*} + \left(E_{ba} + E_4\right) I_2{}^{*}\right] \quad (3.45)$$

$$= I_1{}^2 + a^2 I_2{}^2) R_b + 2aI_1 I_2 R_b \sin\theta$$

Hence, the net power of the air gap developed by the motor is

$$P_{ag} = P_{agf} + P_{agb} \quad (3.46)$$

$$= I_1{}^2 + a^2 I_2{}^2)(R_f - R_b) + 2a(R_f + R_b) I_1 I_2 R_b \sin\theta$$

At standing still, the forward and backward branches have the same rotor impedances. When $R_f = R_b$ in the equation above, the motor's net air-gap power is

$$P_{ag} = 4aI_1 I_2 R_f \sin\theta \quad (3.47)$$

Starting of the motor will be

$$Tst = \frac{2|I_2||I_1|(Rf + Rb)(sin\,(\theta_2 - \theta_1))}{(2\pi Ns)\backslash f} \quad (3.48)$$

$$Tst \approx \frac{|V| R_2'}{(2\pi Ns)[(R_2')^2 + (X_2')^2]} \quad (3.49)$$

The below graph shows the relationship between the torque and the rotor speed of the capacitor-start induction motor. Three different capacitor values were used. 300uF, 180uF, and 100uF capacitors are used. Increasing the capacitance increases the starting torque of the motor, and vice versa. This curve is drawn using MATLAB code in **Appendix (B).**

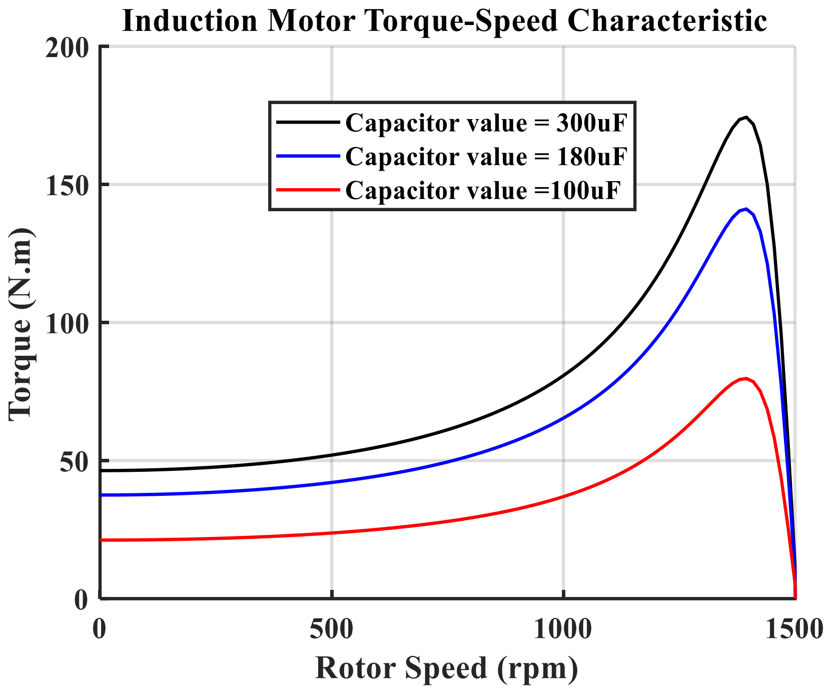

Figure 3.14. A Capacitor-start induction motor's torque-speed characteristic

4. PROPOSED TECHNIQUE

In this study a single-phase induction motor will be derived by using two different voltage sources. One of supply power to the main winding of the motor and the other will supply power to the auxiliary winding. Figure 4.1. represents Single phase induction motor with two different voltage sources. There are three case studies for this thesis. Case study one: SPIM with only the main winding; case study two: SPIM with the main winding and the auxiliary winding with only one voltage source by connecting capacitors in series into the auxiliary winding. Case study three: SPIM with two windings but with two different voltage supplies. **Vm** is the grid voltage that supply power to the main winding where **Va** is the voltage source for the auxiliary winding with variable voltage magnitude and phase angle.

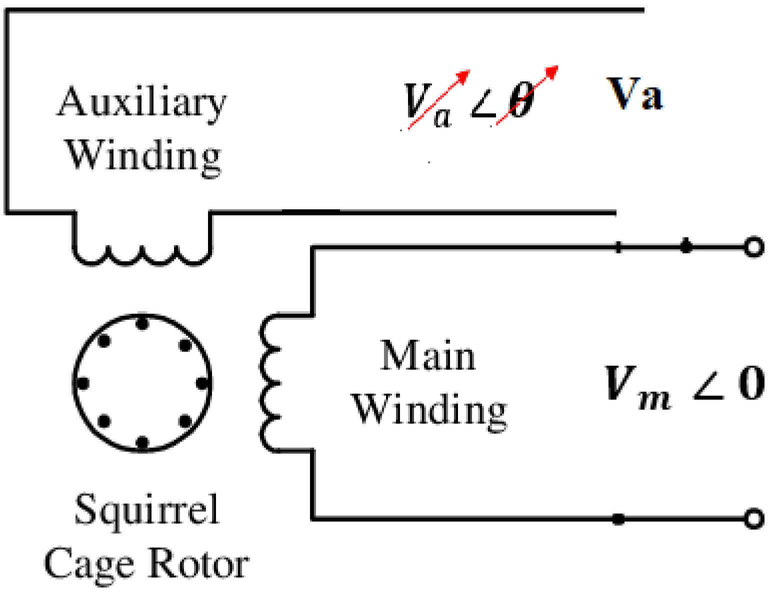

Figure 4.1. Schematic diagram of single-phase induction motor powered by two different voltage sources

4.1. Single phase induction motor parameters

Single-phase induction motor parameters listed in Table 4.5 will be used in this study. These parameters can be divided into three groups. (1) main winding resistance and leakage inductance, (2) auxiliary winding resistance and leakage inductance, and (3) main winding rotor resistance and leakage inductance. This data was taken from model dynamics of single-phase induction motor in MATLAB Simulink.

Table 4.1. Parameters of single-phase induction motor.

No	Parameters	Value
1	Rating	0.25-hp
2	Voltage	220 V
3	Frequency	50Hz
4	Number of poles	4 poles
5	Main winding resistance (Ohm) and leakage inductance (H).	2.02 / 7.4e-3
6	Auxiliary winding resistance (Ohm) and leakage inductance(H).	7.14 / 8.5e-3
7	Main winding mutual inductance (H).	0.1772
8	Main winding rotor resistance (Ohm) and leakage inductance (H).	4.12 / 5.6e-3
9	Capacitor-Start (resistance and capacitor value)	2 / 300e-6
10	Turn ratio	1.18
11	Inertia	0.0146 J(kg.m^2)

4.1.1. Modified equivalent circuits of single-phase induction motor with two sources instead of one.

The equivalent circuit of a single-phase induction motor with two windings that gets power from different voltage sources is illustrated in Figure 4.2. The voltage source that supplies power to the main winding is denoted by (Vm), and the voltage source for the auxiliary winding is denoted by (Va).

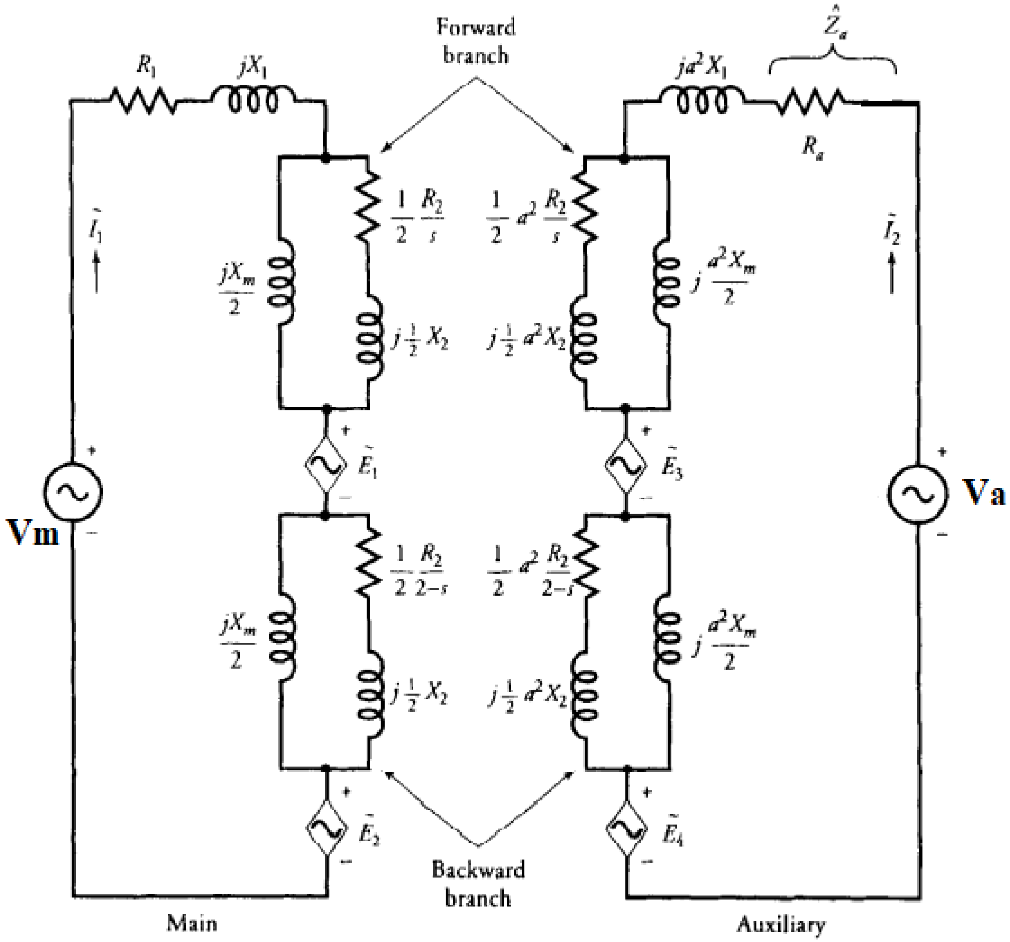

Figure 4.2. Equivalent circuit of the main winding and auxiliary windings of a single-phase induction motor

4.1.1.1. Analysis of a Single-Phase Induction Motor with Varied Phase Angle

A single-phase induction motor with two different voltage sources. one for the main winding and another voltage source for the auxiliary winding. Both the voltage sources have 220 V with a 50 Hz frequency but a different phase angle. The voltage source used for the auxiliary windings has three different phase angles: 0, 30, and 60 degrees. Increasing the phase angle between the main winding and the auxiliary winding increases the starting torque of the motor, as shown in Figure 4.3. The MATLAB code was used for drawing these graphs as shown in **Appendix (C).**

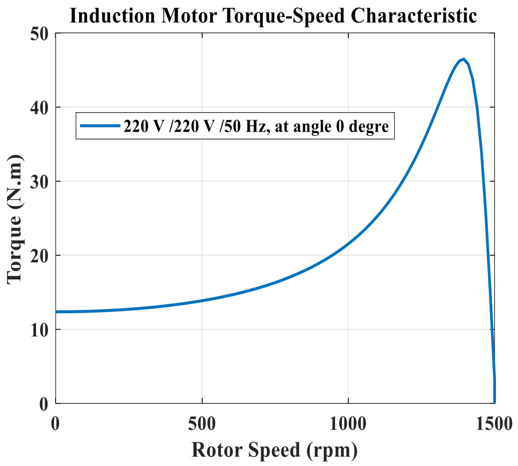

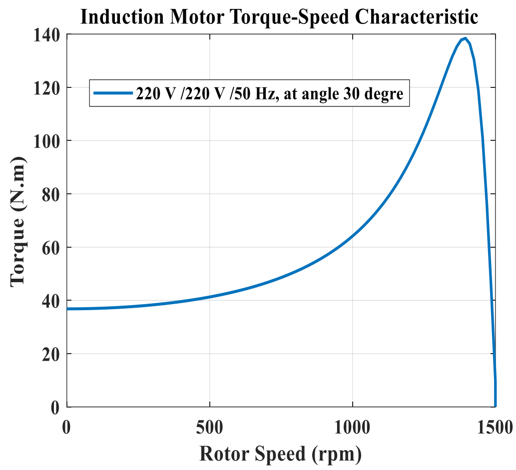

(a) **(b)**

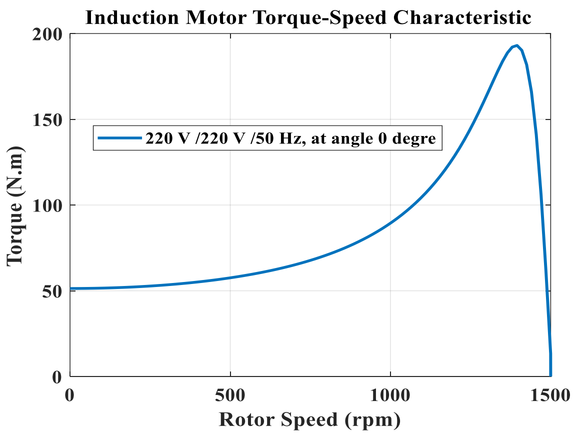

(c)

Figure 4.3. Phase angle between the two windings of the motor; **a)** At angle 0-degrees; **b)** At angle 30-degrees; **c)** At angle 60-degrees

4.1.1.2. Analysis of Single-phase Induction Motor with varied Voltage Magnitude and Phase Angle.

Increasing the phase angle improves the starting torque of the motor. SPIM has a constant main winding voltage, but the magnitude and phase angle of the auxiliary winding voltage are varied. The voltage source for the auxiliary winding has different phase angles; 0, 30, and 60 degrees. Increasing the auxiliary winding voltage is the increasing the starting torque. Figures 4.4 represent the torque speed characteristic curves obtained from the phase shift of the voltage source for the auxiliary winding, respectively.

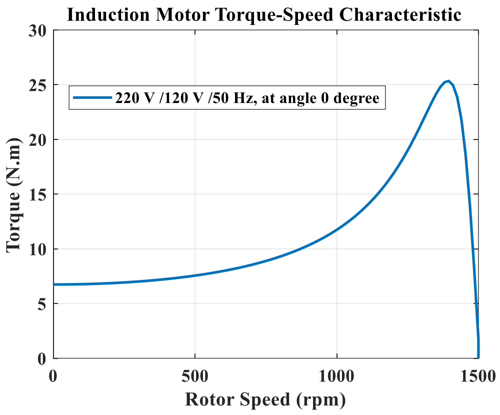

(a)

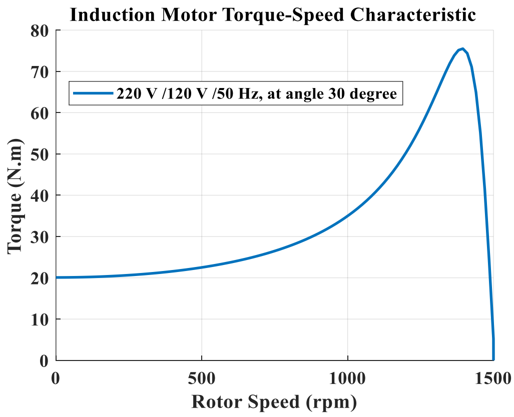

(b)

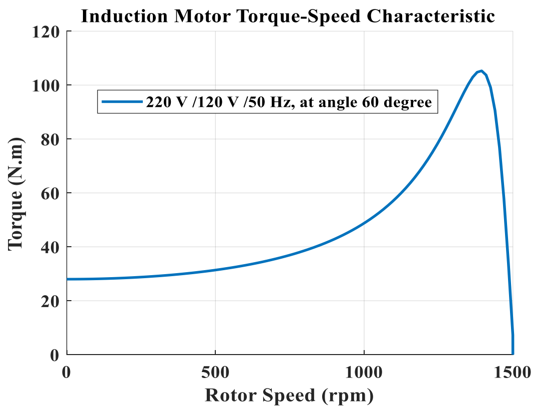

(c)

Figure 4.4. Phase angle between the two windings of the motor; **a)** At angle 0-degrees; **b)** At angle 30-degrees; **c)** At angle 60-degrees

5. RESULTS

The purpose of this study was to improve the starting torque of the single-phase induction motor with two windings (main and auxiliary winding) by using two different voltage sources. In this study, the phase angle between the two voltage sources is controlled to increase the starting torque of the motor and the use of capacitor is eliminated. There are three case studies for this thesis. Case study one: SPIM with only the main winding; case study two: SPIM with the main winding and the auxiliary winding with only one voltage source by connecting capacitors in series into the auxiliary winding. Case study three: SPIM with two windings but with two different voltage supplies. SPIM torque speed characteristic with only one winding is shown in Figure 5.1. This means there is no rotation for the motor because there is no starting torque. Figure5.1b represents the torque speed characteristics for the capacitor start induction motor; here the motor is running or rotating because there is starting torque. Figure5.1c illustrates the torque speed characteristics of proposed study. In this last case study, the motor has starting torque and is in running condition. Case study three: the angle between the two voltage sources can be controlled to improve the starting torque of the SPIM.

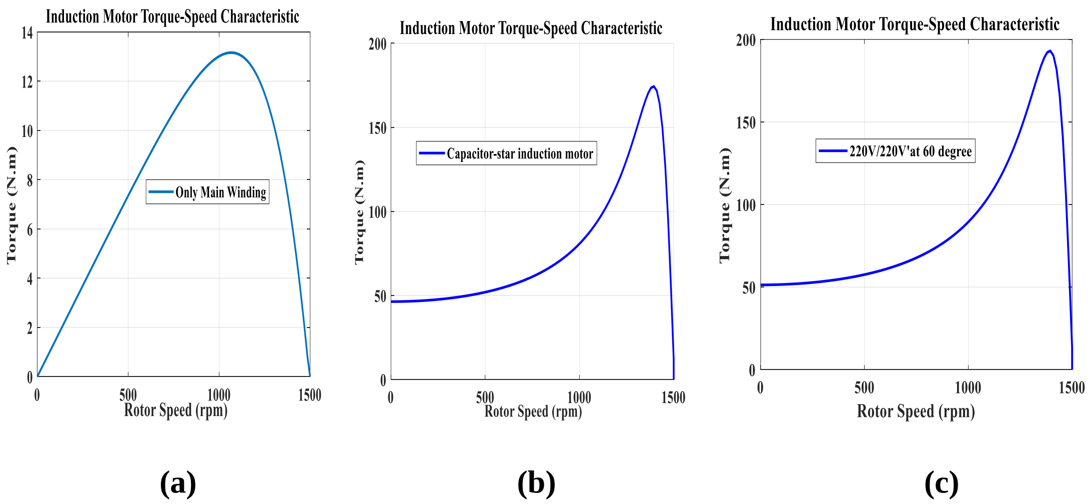

Figure 5.1. Torque speed characteristics of SPIM; **a)** SPIM with only main winding; **b)** Capacitor-star SPIM; **c)** SPIM with two voltage sources

The ability to improve or increase the starting torque of the single-phase induction motor depends on the phase angle between the main winding current and auxiliary winding current. Controlling the phase angle of the voltage source for the auxiliary winding effects the angle between the two currents (the main winding and the auxiliary winding current). Also, the increasing voltage supply for the auxiliary winding increases the starting torque of the SPIM. Figures 5.2a and 5.2b illustrate the torque speed characteristic curves by controlling the phase angle and the voltage source for the auxiliary winding, respectively. The summaries of the relationship between torque angle and voltage source for the auxiliary winding are in Table 5.1.

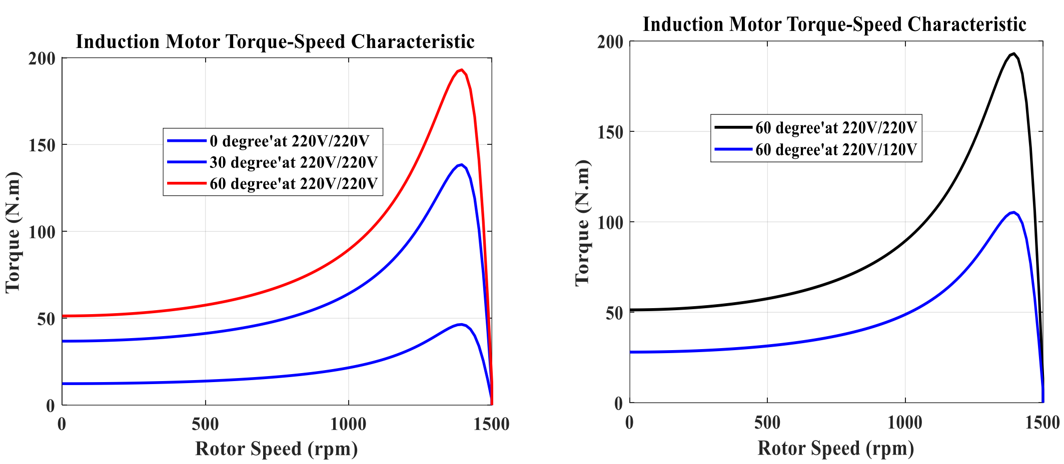

a) b)

Figure 5.2. Torque speed characteristics of SPIM **a)** By controlling the phase angle; b) By controlling the voltage supply for the auxiliary winding

The main winding voltage is set at 220V and varying the auxiliary winding voltage magnitude and phase angle produced many torque speed curves. Table 5.1 summarizes the results of the proposed study in terms of starting torque.

Table 5.1. Relationship between torque, voltage, and the phase angle of the single-phase induction motor

PHASE SHIFT (Degree)	STARTING- TORQUE at 220V / 220V / 50 Hz	STARTING-TORQUE at 220 V / 120V / 50 Hz
0	12.36	6.73
30	36.81	20.08
60	42.12	28.00

6. CONCLUSION

Single-phase induction motors SPIMs are widely used in both commercial and home applications. Single-phase induction for water pumping purposes is also used in rural areas where there is no electrical network. SPIM has a single winding does not start by itself. It can be changed to a two-phase motor at starting to allow it to start by itself. This can be achieved by adding an additional "starter winding," also called the auxiliary winding. There are different methods used to improve the SPIM starting torque characteristic. One of the most known methods for the improving SPIM starting torque are capacitors. The life span is limited for the capacitors, and the replacement of capacitors is difficult in rural areas. That is one of disadvantages of using capacitors. In this study, two inverters were used to drive and improve the torque characteristic of the SPIM, and the use of capacitors is eliminated. The phase angle between the two inverters is controlled to meet the desired starting torque. With this thesis, it provides improvements in torque speed curves. The energy provided by the motor can be from PV panels, wind generators, or an electrical network. A MATLAB program was used for simulation in this study.

7. REFERENCES

Ahmed, T.A., Ali, A.I., Youssef, A. and Mohamed, E.E. 2018. "Study of Multilevel Inverter Fed Single Phase Induction Motor." *2018 Twentieth International Middle East Power Systems Conference (MEPCON),*. cairo: cairo university. 5.

Al-Rubaye, M.J.M., Gino Morais Araujo, V., Kadhim Abed, J. and Van den Bossche, A. 2018. "Review different types of MPPT techniques for photovoltaic systems." *International Conference on Sustainable Energy and Environment Sensing (SEES 2018).* 6.

Amarnath, R. K., and Deepak Verma. 2017. " Modeling and Simulation of Solar Photovoltaic Application Based Multilevel Inverter with Reduced Count Topology for Stand-alone System." *." Electrical & Computer Engineering: An International Journal (ECIJ) 6* 12.

Anwari, Oi, A., M. and Taufik, M., 2009. 2009. "Modeling and simulation of photovoltaic water pumping system." *Third Asia International Conference on Modelling & Simulation* 497-502.

Ashish, K.D, Anil, K.M and Saini. 2017. "Performance Analysis of Single Phase Induction motor with Solar PV Array for water Pumping." *International Journal of Engineering Research & Technology (IJERT)* 7.

Bai, Ying, and Dali Wang. 2006. ". "Fundamentals of fuzzy logic control—fuzzy sets, fuzzy rules and defuzzifications." Advanced fuzzy logic technologies in industrial applications. ." *Springer, London,* 17-36.

Bhattacharya, S. K. (2011). Control Systems Engineering: . Indi: JNTU. Pearson Education Indi.

Bhattacharya, S.K.,. (2011). Control Systems Engineering:. Indi: JNTU. Pearson Education Indi.

Bunty B. B, Dakshata U. K. 2012. *solarword.blogspot.* 11 1. http://solarword.blogspot.fi/2012/11/explaining-working-principle-of.html [01.11.2012].

Chapman, S.J.,. 2012. *Electric machinery fundamentals fifth edition.* newyork: McGraw-Hill.

Chapman, Stephen J. "Electric machinery fundamentals fifth edition." (2012). 2012. *Electric machinery fundamentals fifth edition.* newyork: McGraw-Hill.

Eltawil, Mohamed A., and Zhengming Zhao. . 2013. ""MPPT techniques for photovoltaic applications." Renewable and sustainable energy reviews 25 (2013): 793-813." *Renewable and sustainable energy reviews 25 (2013* 22.

Foito, D., Guerreiro, M. and Pires, V.F.,. 2014. "Single-phase induction motor controller for photovoltaic powered water pump." *2014 16th International Power Electronics and Motion Control Conference and Exposition. IEEE,.* Antalya, Turkey: International Power Electronics and Motion Control Conference and Exposition. 6.

Ganesh, E. N. 2017. "Design of Inverter Using Sinusoidal Pulse Width Modulator in DSP Processor."." *International Journal of Analog Integrated Circuits* 7.

Gonen, T. 2011. *Electrical Machines with MATLAB®. CRC press.* Boca Raton, Florida, United States: CRC press.

Gonen, T.,. 2011. *Electrical Machines with MATLAB®.* . Boca Raton, Florida, United States: CRC press.

Gupta, K.K. and Bhatnagar, P.,. 2017. Multilevel inverters: conventional and emerging topologies and their control. Cambridge, Massachusetts: Academic Press.

Hart, D. W., & Hart, D. W. 2011. *Power electronics (Vol. 166).* McGraw-Hill.: New York.

Ilango, G. Saravana, and N. Rajasekar. 2009. "An improved energy saving v/f control technique for solar powered single-phase induction motor." Energy conversion and Management ." *elsevier* 2913-2918.

Iqbal, A., Moinoddin, S., & Reddy, B. P. 2021. Electrical Machine Fundamentals with Numerical Simulation using *MATLAB SIMULINK.* USA: John Wiley & Sons Ltd.

Karami, Nabil, Nazih Moubayed, and Rachid Outbib. 2017. " General review and classification of different MPPT Techniques." *" Renewable and Sustainable Energy Reviews 68 (2017): 1-18* 18.

Kumar, S.S.K. and Dhal, P.K. 2015. "Analysis of dynamic performance based inverter fed single phase induction motor." *2017 4th International Conference on Advanced Computing and Communication Systems (ICACCS).* coimbatore, india: 2017 4th International Conference on Advanced Computing and Communication Systems (ICACCS). 7.

Mittal, V. M. A. 2004. Basic Electrical Engineering. newyork: Tata McGraw-Hill. .

Mohamed. 2015. *Author: Mohamed Amer Chaaban,.* 2 5. Accessed 2 5, 2015. https://www.e-education.psu.edu/ae868/node/518.

Muhammad, R. H. (2014). Power Electronics Devices, Circuits and Applications.*" (2014).* london: pearson.

Muhammad, R.H., Narendra, K. and Ashish, R.K. 2014. *Power Electronics Devices, Circuits,and Applications.* india: pearson.

Nandha kumar, A. , Senthilkumar, R. , Alex Stanley Raja,T. and Santhoshkumar K.V. 2019. "Photo Voltaic Powered Voltage Source Inverter for Single Phase Induction motor with MPPT Algorithm." *International Journal of Innovative Technology and Exploring Engineering (IJITEE)* 6.

Noman, Abdullah M., Khaled E. Addoweesh, and Hussein M. Mashaly. 2012. "A fuzzy logic control method for MPPT of PV systems." *" IECON 2012-38th Annual Conference on IEEE Industrial Electronics Society. IEEE, 2012* 7.

Ogudo, Kingsley A., and Josias W. Makhubele. 2019. ""Comparative Analysis on Modulation Techniques For A Single Phase Full-Bridge Inverter on Hysteresis Current Control PWM, Sinusoidal PWM and Modified Sinusoidal PWM." ." *2019 International Conference on Advances in Big Data, Computing and Data Communication Systems (icABCD).* 7.

Peddapelli, S.K.,. 2016. Pulse width modulation: analysis and performance in multilevel inverters. berlin: Walter de Gruyter GmbH & Co KG,.

Rao, R. Kameswara, P. Srinivas, and MV Suresh Kumar. 2014. "design and analysis of various inverters using different PWM techniques." .*The International Journal of Engineering And Science (IJES).* 10.

Rashid, M. ed.,. 2014. Alternative energy in power electronics. Oxford: Butterworth-Heinemann.

Rezk, Hegazy, and Ali M. Eltamaly. 2015. ""A comprehensive comparison of different MPPT techniques for photovoltaic systems." *Solar energy 112* 11.

Sahoo, Sarat Kumar, et al.. (2012). ""Performance analysis and simulation of three phase voltage source inverter using basic PWM techniques." *Chennai and Vivekanandha College of Technology for women, Th ird International Conference on Sustainable Energy and Intelligent System.* india: VCTW, Tiruchengode, Tamilnadu,. 257-263.

Saini, A.K. and Dubey, A.K. 2017. "Performance Analysis of Single Phase Induction motor with Solar PV Array for water Pumping." *International Journal of Engineering Research & Technology* 721-727.

Sen, P.C. 2007. Principles of electric machines and power electronics. *John Wiley & Sons.* new york: John Wiley & Sons.

Sen, Paresh Chandra. 2014. Principles of electric machines and power electronics. *John Wiley & Sons,* . Hoboken, New Jersey: John Wiley.

Senty, S. 2012. *Motor Control Fundamentals.* Boston, Massachusetts, United States: Cengage Learning,.

Solanki, C.S. 2013. Solar photovoltaic technology and systems: a manual for technicians, trainers and engineers. New Delhi: PHI Learning Pvt. Ltd.

Thomas, A.R. and Mathew, S,. 2014. "Solar powered single phase induction motor using single source five level inverter." *Annual International Conference on Emerging Research Areas: Magnetics, Machines and Drives (AICERA/iCMMD).* 6.

Ugale, J.H. and Panse, M.S.,. 2015. "Single phase AC drive for isolated solar photovoltaic water pumping system." *2015 International Conference on Green Computing and Internet of Things (ICGCIoT).* india: International Conference on Green Computing and Internet of Things (ICGCIoT).

Vtas, P. and Pal, Y.,. 2017. "Solar PV Array Buck-Boost Converter Fed Single Single Induction Motor Drives for Water Pumping." *International Conference on Information, Communication, Instrumentation and Control (ICICIC)* 5.

Wildi, T.,. 2014. *Electrical machines, drives, and power systems.* London: pearson.

Youssef, M., Boubahri, C., Fetni, S., & Aloui, F. (2020). "Simulation and design of a single phase inverter with digital PWM issued by an Arduino board." *ResearchGate. doi, 10.* 9.

Zekry, A., Shaker, A. and Salem, M. 2018. "Solar cells and arrays: Principles, analysis, and design." Advances in renewable energies and power technologies." *Elsevier*, 3-56.

8. APPENDIXS

Appendix (A)

```
clear all
   close all
   clc
V = 220;
R1 = 2.02;
X1 = 2.32;
XM = 55.64;
R2 = 4.12;
X2 = 1.7584;
P = 4 ;
Fz = [50:10:60];
for i = length(Fz)
for x = 1:1
w_sync = (4*pi*Fz(x))/P;
n_sync = (120*Fz(x))/P;
s = 0:0.01:1;
s(1) = 0.0001;
nm = (1-s).*n_sync;
ZFrw = ((R2./s)+j*X2).*(j*XM)./((R2./s)+j*X2+(j*XM));
ZBwr = ((R2./(2.-s))+j*X2).*(j*XM)./((R2./(2.-s))+j*X2+(j*XM));
I1 = V./ (R1+j*X1+0.5*ZF+0.5*ZB);
PAGFrw = (abs(I1)).^2.*(0.5*real(ZFrw));
PAGBrw = (abs(I1)).^2.*(0.5*real(ZBrw));
PAG = PAGFrw - PAGBrw;
Tind = PAG./w_sync;
end
end
plot(nm,Tind,'LineWidth',2.0)
```

Appendix (B)

```
clear all
   close all
   clc
Vm = 220 ;
Va = 220 ;
C = 180e-6;
R1m = 2.02;
X1m = 2.32;
R1a = 7.14;
X1a = 2.669;
XM = 55.64;
M5 = abs(XM)
R2 = 4.12;
```

```
X2 =1.7584;
a = 1.18;
w_sync = 188.5;
n_sync = 1500;
s = 0:0.01:1;
s(1) = 0.0001;
nm = (1-s).*n_sync;
Zff = ((0.5*R2)+j*X2*0.5).*(j*XM*0.5)./((0.5*R2)+j*X2*0.5+(j*XM*0.5));
Zm=R1m+j*X1m+2*(((0.5*R2)+j*X2*0.5).*(j*XM*0.5)./((0.5*R2)+j*X2*0.5+(j*XM
*0.5)));
M1 =abs(Zm)
Xc = 1/(2*pi*50*C);
Zc = -j*Xc;
Rff= ((M1) -R1m)/2;
Rbb = Rff ;
Za = R1a+j*(X1a -
Xc)+2*(((0.5*R2)+j*X2*0.5).*(j*XM*0.5)./((0.5*R2)+j*X2*0.5+(j*XM*0.5)));
Z1m = R1m+(j*X1m);
Z1a = R1a+j*X1a;
Im = (Vm/Zm);
M2 = abs(Im)
Ph1 = angle(Im)
Ia = ((Vm)/Za);
M3 = abs(Ia)
Ph2 = angle(Ia)
alpha = (Ph2-Ph1);
Ist = (Im +Ia);
IstM = abs(Ist)
ZF = ((R2./s)+j*X2).*(j*XM)./((R2./s)+j*X2+(j*XM));
RF = real(ZF);
ZB = ((R2./(2.-s))+j*X2).*(j*XM)./((R2./(2.-s))+j*X2+(j*XM));
RB = real(ZB);
Zin = ZF+ZB+R1m +j*X1m;
Iin = (Vm\Zin);
M8 =abs(Iin)
Tst = (((2*a*M2*M3)*(RF+RB))*sin(Ph2-Ph1))/((2*pi*n_sync)/50);
plot(nm,Tst)
```

Appendix (C)

```
Vm = 220 ;
Va = 220 ;
R1m = 2.02;
X1m = 2.32;
R1a = 7.14;
X1a = 2.669;
XM = 55.64;
M5 = abs(XM)
```

```
R2 = 4.12;
X2 =1.7584;
Z1m = R1m+(j*X1m);
Z1a = R1a+j*X1a;
a = 1.18;
w_sync = 188.5;
n_sync = 1500;
s = 0:0.01:1;
s(1) = 0.0001;
nm = (1-s).*n_sync;
Zm =
R1m+j*X1m+2*(((0.5*R2+j*X2*0.5).*(j*XM*0.5))./(0.5*R2+j*X2*0.5+j*XM*0.5));
M1 =abs(Zm)
Za = R1a+j*X1a
+(2*((0.5*R2+j*X2*0.5).*(j*XM*0.5)./(0.5*R2+j*X2*0.5+j*XM*0.5)));
Im = (Vm/Zm);
M2 = abs(Im)
Ph1 = angle(Im)
Ia = ((Va)/Za);
M3 = abs(Ia)
Ph2 = angle(Ia)
alpha = (Ph2-Ph1);
Ist = (Im +Ia);
IstM = abs(Ist)
ZF = ((R2./s)+j*X2).*(j*XM)./((R2./s)+j*X2+(j*XM));
RF = real(ZF);
ZB = ((R2./(2.-s))+j*X2).*(j*XM)./((R2./(2.-s))+j*X2+(j*XM));
RB = real(ZB);
Zin = ZF+ZB+R1m+j*X1m;
Iin = (Vm\Zin);
M8 =abs(Iin)
Tst = (((2*a*M2*M3)*(RF+RB))*0.0000175)/((2*pi*n_sync)/50);
plot(nm,Tst,'LineWidth',2.0)
```

BACKGROUND

MUSTAFE ADEN MUHUMED

Mustafa.gabyaye@gmail.com

EDUCATIONAL INFORMATION

Master Degree 2019-2022	Akdeniz university Electrical and Electronic Department of Engineering, Antalya, TURKIYE
Bachelor Degree 2013-2018	University of Hargeisa Electrical and Electronic Department of Engineering, Hargeisa, SOMALIA.